

# Experimental investigation of nitrogen species release from different solid biomass fuels as a basis for release models

Gerhard Stubenberger<sup>a,\*</sup>, Robert Scharler<sup>a,b,c</sup>, Selma Zahirović<sup>a,b</sup>,  
Ingwald Obernberger<sup>a,b,c</sup>

<sup>a</sup> Austrian Bioenergy Centre GmbH, Inffeldgasse 21b, A-8010 Graz, Austria

<sup>b</sup> Institute for Resource Efficient and Sustainable Systems, Graz University of Technology, Inffeldgasse 21b, A-8010 Graz, Austria

<sup>c</sup> BIOS BIOENERGIESYSTEME GmbH, Inffeldgasse 21b, A-8010 Graz, Austria

Received 18 December 2006; received in revised form 4 May 2007; accepted 10 May 2007

Available online 14 June 2007

## Abstract

Experimental data on the release of NO<sub>x</sub> precursors from solid biomass fuels during thermal conversion are necessary to study N release in general and to supply reliable data for the purpose of packed bed and gas phase conversion model development and validation. In this work the release of NO<sub>x</sub> precursors was studied at a lab-scale pot furnace (batch reactor) by taking measurements during the conversion process of solid biomass in a packed bed. The investigations were carried out with relevant woody biomass fuels, which cover a broad range of fuel N contents: sawdust, bark, waste wood and MDF board. The most important NO<sub>x</sub> precursor detected above the fuel bed under fuel rich conditions was NH<sub>3</sub>, while HCN was almost insignificant with the exception of sawdust. NO was detected mainly under air rich conditions. Furthermore, the experimental data were utilised to derive release functions for the relevant NO<sub>x</sub> precursors NO, NH<sub>3</sub> and HCN. The release functions were implemented in an in-house empirical packed bed combustion model, which serves as a basis for a subsequent CFD N species gas phase calculation.

© 2007 Elsevier Ltd. All rights reserved.

**Keywords:** Biomass; Combustion; Nitrogen release; Nitrogen release modelling; NO<sub>x</sub> precursors

## 1. Introduction and objectives

Lowering NO<sub>x</sub> emissions is one of the crucial issues of thermal biomass utilisation. As N species formation during combustion of solid biomass fuels is a very complex process, the design of low-NO<sub>x</sub> furnaces is still mainly based on experience in most cases. Therefore, model based design tools, e.g. CFD (computational fluid dynamics) calculation of N release, are necessary. Fundamental experimental investigations of the release behaviour of relevant NO<sub>x</sub> precursors (HCN, NH<sub>3</sub>, NO, NO<sub>2</sub> and N<sub>2</sub>O) from solid

biomass fuels are necessary as a basis for model development since the major part of available scientific work was performed on coal combustion and there is thus a need for reliable data concerning the conversion of solid biomass in grate furnaces [1–3].

The three main sources for NO<sub>x</sub> emissions during combustion are thermal, prompt and fuel NO<sub>x</sub>. In the case of biomass combustion the only relevant source is the conversion of fuel bound N because the high temperatures (>1300 °C) at which thermal and prompt NO<sub>x</sub> formation paths become active are rarely achieved during solid biomass combustion [1,4,5]. The conversion of fuel N follows the simplified reaction path shown in Fig. 1.

The release of fuel N during the thermal decomposition of solid biomass fuels is a very complex process. Fuel N is released partly during pyrolysis as volatiles while the remaining part is released during charcoal burnout.

\* Corresponding author. Tel.: +43 0316 873 9201; fax: +43 0316 873 9202.

E-mail address: [gerhard.stubenberger@abc-energy.at](mailto:gerhard.stubenberger@abc-energy.at) (G. Stubenberger).

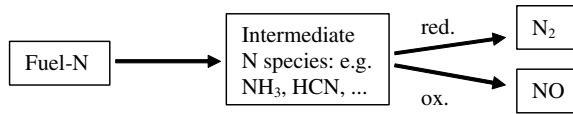


Fig. 1. Simplified scheme of the conversion of fuel bound N during biomass combustion.

However, N release is dependent on the temperature, heating rate, particle size and fuel type [1,2,6–9] in the case of fluidised bed combustion, for example. The relevant N species released from the fuel bed on a grate are  $\text{NH}_3$ , HCN, NO,  $\text{NO}_2$ ,  $\text{N}_2\text{O}$  and  $\text{N}_2$  [3,5,10–13]. The influencing parameters reported in available studies include the air ratio, temperature, residence time and fuel N content. The N species formed during pyrolysis are mainly HCN,  $\text{NH}_3$ , HNCO and tar N, whereas their fractions depend on the fuel type, the temperature, the heating rate and the fuel O/fuel N ratio [1,6,7,9,10]. Char N is released mainly as NO and  $\text{N}_2$  [1,8,10].

Due to lack of reliable data on the N species release behaviour from solid biomass fuels during grate combustion, test runs were performed at an in-house lab-scale pot furnace. The fuels selected for the experiments covered a broad range of relevant woody biomass fuels (sawdust, bark, waste wood and MDF board) [14,15] with varying nitrogen concentrations.

The experimental investigations of the selected woody biomass fuels provided the basis for deriving N species release functions for  $\text{NO}_x$  precursor release. The fitting procedure is based on a previous work by Widmann [16]. The function parameters were derived by approximation of the profiles of the N flue gas species measured. The measured and calculated N flue gas species release profiles and N flue gas species conversion rates were compared. These release functions form an important basis for CFD calculations of N release in biomass grate furnaces since they can provide the boundary conditions for the subsequent CFD

gas phase calculations concerning N flue gas species (for further details see [15,17]).

## 2. Methodology

This chapter describes the lab-scale pot furnace and the experimental setup and introduces the empirical packed bed combustion model and the implemented N species release model. Finally, the procedure for the derivation of the N species release functions is outlined.

### 2.1. Pot furnace experiments

The lab-scale reactor (see Fig. 2) is a discontinuously operated cylindrical pot furnace reactor. The lab-scale pot furnace was designed in a manner so as to represent the burning packed bed of biomass in a grate furnace as accurately as possible. The applicability of the lab-scale pot furnace results to grate furnaces is based on the following assumptions: (1) the speed of the packed bed on the grate is constant, (2) the diffusional transport and mixing effects in the direction of the grate can be neglected compared to the transport of the fuel along the grate and hence, (3) in dependence on a certain residence time, any particle can be related to a position on the grate according to the conversion progress.

The fuel is placed in a sample holder, which rests on a balance. Electrically heated elements are installed in order to heat-up and ignite the fuel sample by radiation. The fuel sample holder is inserted into the reactor as soon as a certain reactor temperature is achieved.

Several thermocouples are installed inside the fuel bed in order to measure the temperature at different heights. Combustion air is introduced through a porous plate on which the fuel bed rests. In order to avoid the penetration of false air, the reactor is sealed with thermal oil. There are two channels in the upper part of the retort, which allow gas phase concentrations of  $\text{H}_2\text{O}$ ,  $\text{CH}_4$ , CO,  $\text{CO}_2$  and

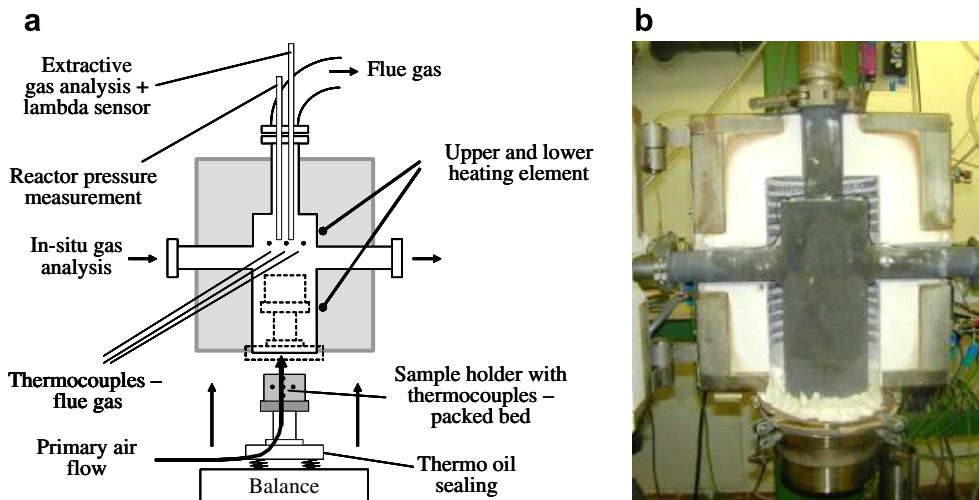


Fig. 2. Scheme of the experimental setup (a) and picture of the lab-scale pot furnace (b).

NH<sub>3</sub> to be measured just above the fuel bed using a specially developed hot gas in situ FTIR technique [18]. Three thermocouples are placed above the sample holder to measure the temperature of the flue gas leaving the fuel bed. Furthermore, the difference between ambient and reactor pressure is detected for the purpose of correcting the data gained by the weight measurements (causing additional forces acting on the balance). In addition, extractive gas measurements were performed using a heated suction probe in order to sample the flue gas right above the fuel bed. The gas stream sampled was analysed for CO, CO<sub>2</sub>, H<sub>2</sub>O, CH<sub>4</sub>, C<sub>2</sub>H<sub>6</sub>, C<sub>2</sub>H<sub>4</sub>, C<sub>2</sub>H<sub>2</sub> and some further hydrocarbons as well as NO, NH<sub>3</sub>, HCN, NO<sub>2</sub> and N<sub>2</sub>O using extractive FTIR (Gasmeter™ DX-4000). The extractive FTIR device was calibrated by means of daily background spectra of pure N<sub>2</sub>. The extracted gas stream was diluted with N<sub>2</sub> in order to avoid further reactions, condensation of water and hazardous concentrations of the flue gas species. The dilution factor was maintained at a ratio of about 1:12, which was controlled by the pressure of N<sub>2</sub> supplied to the dilution unit during the test runs. The dilution factor was determined by measuring the oxygen concentration of air with and without dilution before every measurement campaign. Furthermore, the gas stream sampled was analysed for H<sub>2</sub>, NO, O<sub>2</sub>, CO and CO<sub>2</sub> using conventional gas analysers, which were calibrated by means of test gases with defined concentrations before every measurement campaign. In addition, information about the stoichiometric air ratio in the flue gas was gained by means of a wide-band ZrO<sub>2</sub> sensor, which also provided the basis for determining the concentrations of oxygen in the flue gas. A three point calibration of the lambda sensor (air, N<sub>2</sub> and 20 vol% CO in N<sub>2</sub>) was performed in order to calibrate the lambda sensor before every measurement campaign. The element balances for each pot furnace experiment were calculated based on the measurement data. The test runs showed the extractive FTIR (more flue gas species detectable and smaller measurement errors) results to be more accurate than those obtained by in situ FTIR, and therefore only the results of the extractive FTIR measurements were utilised for this paper. A more detailed description of the lab-scale reactor can be found in [12,16].

The experimental conditions for all test runs performed are summarised in Table 1. The different sample masses of the fuels investigated can be explained by the difference in fuel densities, since the sample holder was always com-

pletely filled. In the case of sawdust the mass flow of air had to be reduced from 0.0832 to 0.0544 kg/m<sup>2</sup> s in order to avoid particle entrainment from the fuel bed due to the small particle sizes.

## 2.2. Description of the existing empirical packed bed combustion model including N release

An empirical model was developed for the combustion of solid biomass on a grate [19]. This model supplies velocity profiles, species concentration profiles (CH<sub>4</sub>, CO, CO<sub>2</sub>, H<sub>2</sub>, H<sub>2</sub>O, O<sub>2</sub> as well as NH<sub>3</sub>, HCN and NO) and temperature profiles of the flue gas above the surface of the fuel layer as boundary conditions for the subsequent gas phase CFD simulation of the reacting flow in the furnace [17]. In this model the fuel bed is divided into small slices for which mass and energy balances are solved. The model follows a three-step approach.

The first step covers the decomposition of the biomass fuel and the release of the fuel components C, H, O, N and H<sub>2</sub>O. Pre-defined 1D elemental release profiles along the grate are used, which were derived from experiments at the pot furnace and a grate furnace [19]. The second step covers the conversion of the fuel components to the flue gas species CO<sub>2</sub>, CO, H<sub>2</sub>O, O<sub>2</sub>, H<sub>2</sub> and CH<sub>4</sub> using functions that are dependent on the stoichiometric air ratio in the fuel bed  $\lambda_{\text{fuel bed}}$  at the present state of the model. Steps one and two allow for a discrete balancing of mass and energy fluxes released from the fuel bed along the grate (step 3). A more detailed description of the model can be found in [15,16,19].

The release of N containing species from the fuel bed was also modelled according to the steps one to three. The conversion of fuel N to gaseous N species shows strong dependencies on the stoichiometric air ratio in the fuel bed  $\lambda_{\text{fuel bed}}$ , the fuel N content and the kind of fuel used. The conversion functions for NH<sub>3</sub>, NO and HCN were thus derived as a function of  $\lambda_{\text{fuel bed}}$  and are valid for a certain fuel type with a given fuel N content according to the results achieved from the release tests for sawdust, bark, waste wood and MDF board. The principle of the conversion functions was derived in a previous work [16] based on experimental data from Keller [5] and own data. In the experimental data, conversion rates of NO, NH<sub>3</sub> and HCN were correlated to different values of  $\lambda_{\text{fuel bed}}$ . This measurement data could be approximated with a reasonable accuracy by a linear function for the conversion rate  $u_i$  of N species  $i$  [16], which is:

$$u_i = k_i \lambda_{\text{fuel bed}} + d_i [-], \quad (1)$$

where  $k_i$  is the slope,  $\lambda_{\text{fuel bed}}$  the stoichiometric air ratio and  $d_i$  the  $y$ -intercept.  $\lambda_{\text{fuel bed}}$  is given by

$$\lambda_{\text{fuel bed}} = \frac{n_{\text{O, available}}}{n_{\text{O, stoichiometric}}} [-], \quad (2)$$

Table 1  
Experimental conditions for the lab-scale reactor measurements

Fuel	Oxidising medium	Mass flow of air (kg/m <sup>2</sup> s)	Heating elements		Sample mass (g)
			upper (°C)	lower (°C)	
Sawdust	Air	0.0645	750	450	106
Bark	Air	0.0832	750	450	158
Waste wood	Air	0.0832	750	450	107
MDF board	Air	0.0832	750	450	155

where  $n_{O, \text{available}}$  is the local amount of total oxygen available in the fuel bed and  $n_{O, \text{stoichiometric}}$  is the oxygen needed for a complete combustion of the converted fuel.

The conversion rates  $u_i$  of all species were limited by setting the limits  $u_{i, \text{min}}$  (typically 0%) and  $u_{i, \text{max}}$  (typically 100%) in order to avoid non-physical values. If the sum of the conversion rates of NO, NH<sub>3</sub> and HCN is higher than 100%, a normalisation to 100% is performed as a subsequent step. When the sum of the conversion rates for the NO<sub>x</sub> precursors is smaller than 100%, the difference is assumed to be N<sub>2</sub>.

Only NH<sub>3</sub>, NO and HCN are considered by the model at present because these species are the most relevant ones, as observed during previous pot furnace experiments. Other possible NO<sub>x</sub> precursors such as NO<sub>2</sub> and N<sub>2</sub>O have not been included in the model so far, since previous experiments showed that the concentrations of these compounds above the fuel bed are very low for the fuels investigated (for further details see [15,17,19]). HNCO was not studied in this work due to the lack of reference data for the FTIR equipment used. However, HNCO was found in a recent study [9] to be released during pyrolysis in a fluidised bed reactor, but only in small quantities (for further explanations see Chapter 3.1.3).

### 2.3. Derivation of release functions for relevant N species

The results of the test runs at the lab-scale reactor were evaluated in order to derive the parameters of the release functions for the relevant N containing flue gas species. The data used for calculating the release function parameters are release profiles over time for carbon, hydrogen, oxygen and nitrogen as well as concentration profiles over time and total conversion rates for NO, NH<sub>3</sub> and HCN. These release profiles over time were derived from the elemental mass balances calculated for each test run. The total conversion rate  $u_{i, \text{total}}$  of a flue gas species  $i$  (e.g. NO) is calculated as follows:

$$u_{i, \text{total}} = \frac{m_{N, i, \text{flue gas}}}{m_{N, \text{fuel sample}}} (\text{wt}\%), \quad (3)$$

where  $m_{N, i, \text{flue gas}}$  is the mass of N contained in the flue gas species  $i$  detected and  $m_{N, \text{fuel sample}}$  is the mass of N contained in the fuel sample.

The first step of the derivation procedure was the averaging of the results from the test runs performed under the same combustion conditions (amount of combustion air, pre-heating temperature of the reactor and oxygen content of the oxidising medium) for each fuel. The release profile for carbon was then deduced by a cumulative subtraction of all C containing flue gas species detected from the initial amount of C contained in the fuel sample. Subsequently, this release profile was fitted by a polynomial equation. Carbon, the most relevant fuel component, was chosen to define a reference profile for the other fuel components. It is important to note that a good agreement between the calculated and measured carbon release

profiles was essential for the fitting procedure because this profile forms the basis for the release profiles of the fuel components calculated with the empirical combustion model. Based on these release profiles and the profile of the oxidising medium supplied, the stoichiometric air ratio in the fuel bed  $\lambda_{\text{fuel bed}}$  is calculated over time according to Eq. (2). Furthermore, according to the assumptions of the lab-scale reactor (described in chapter 2.1), the measured and calculated profiles of  $\lambda_{\text{fuel bed}}$  were compared qualitatively. However, since the measured value is based on the flue gas species detected in the sampled flue gas stream (without tars and higher hydrocarbons) it is always slightly higher than the calculated value, where tars and hydrocarbons are considered as CH<sub>4</sub>. Deviations between the calculated and measured  $\lambda_{\text{fuel bed}}$  values could also be due to slight differences between the calculated and measured release profiles of C, H, O and N. The last step consisted of fitting the parameters for the release functions (Eq. (1)) of fuel N converted into NO, NH<sub>3</sub> and HCN. The parameters were fitted until the predicted N species concentration profiles and N species conversion rates were in reasonable agreement with the measured results.

## 3. Discussion of results

In this chapter, the experimental results on the combustion and release behaviour of selected woody biomass fuels from lab-scale test runs are presented and discussed with a special focus on N species. Based on these data, N release function parameters were derived for the fuels selected following the procedure described in chapter 2.3.

### 3.1. Experimental results

This section summarises the experimental results of the test runs with sawdust, bark, waste wood and MDF board (for experimental conditions see chapter 2.1; for relevant fuel data see Table 2). The main differences between the fuels considered are fuel N content, particle size distribution and water content. Firstly, the major flue gas species profiles and the mass decrease for bark are discussed as an example in order to give an overview of a complete test run. Secondly, the profiles of the NO<sub>x</sub> precursors and  $\lambda_{\text{fuel bed}}$  are discussed for the individual biomass fuels. Finally the conversion rates for the NO<sub>x</sub> precursors and TFN (total fixed nitrogen; the sum of N species detected with the exception of N<sub>2</sub> – NO, NH<sub>3</sub>, HCN, NO<sub>2</sub> and N<sub>2</sub>O) are discussed for the biomass fuels investigated.

The results were averaged over three test runs for each fuel. The reproducibility of the test runs was good, which is deduced from small standard deviations calculated within the averaging process. The largest deviations between the single test runs occurred due to differences in the point of ignition, caused by, for example, variations in fuel water content or initial sample weight. In general, the combustion behaviour of all fuels investigated was similar, particularly in terms of the conversion stages and the

Table 2  
Relevant data of the biomass fuels used in the lab-scale tests

Fuel	<i>c</i> (wt% d.b.)	<i>h</i> (wt% d.b.)	<i>o</i> (wt% d.b.)	<i>n</i> (wt% d.b.)	<i>w</i> (wt% d.b.)	Range $d_p$ (mm)	Mean $d_p$ (mm)
Sawdust	49.1	6.6	44.2	0.06	<0.1	<3	0.3
Bark	49.5	5.6	40.1	0.27	7.4	1 to 20	3.0
Waste wood	48.2	6.0	43.1	1.00	17.4	1 to 25	2.8
MDF board	46.2	6.6	38.4	6.87	7.5	1 to 40	2.7

*c* – carbon content; *h* – hydrogen content; *o* – oxygen content; *n* – nitrogen content; *w* – moisture content;  $d_p$  – particle diameter; mean  $d_p$  – on the basis of particle number.

major flue gas species profiles. In this context it must be stated that the conversion stages H&D (heat-up and drying), P&G (pyrolysis and gasification) as well as charcoal burnout are partly overlapping in a packed bed and no strict separation is thus possible. However, in the majority of cases one conversion process is dominant for a certain time period.

### 3.1.1. Major flue gas species release and mass decrease for bark as an example

The mass decrease and the profiles of the major flue gas species released during the test runs with bark are illustrated in Fig. 3. Ignition occurred after approximately 200 s, when the H&D conversion stage was over for the greater part of the fuel. The subsequent P&G conversion stage lasted until approximately 600 s. During P&G, the major part of the initial sample mass was converted (see Fig. 3b) and the concentrations of most of the flue gas species (e.g. CO<sub>2</sub> and H<sub>2</sub>O) reached the maximum values (see Fig. 3a). CO, H<sub>2</sub> and CH<sub>4</sub> were also detected in significant concentrations at this stage due to air lean conditions (see Fig. 4d). Lighter hydrocarbons were present only in minor concentrations. After about 600 s charcoal burnout became the dominant conversion stage, releasing mainly CO and CO<sub>2</sub>.

Samuelsson et al. [11] performed test runs for bark and sawdust pellets at a somewhat larger batch reactor and achieved qualitatively similar results for the major flue gas species. However, in the studies of Samuelsson et al. the gas was sampled in the fuel bed, which was probably the reason for significantly higher concentrations of CO.

Zhou et al. [13] studied the release behaviour of straw at a lab-scale experimental rig. In contrast to the present work, however, Zhou et al. measured similar profiles of the major flue gas species above the bed surface at a larger mass flow rate of air. Zhou et al. also detected larger concentrations of CO during the conversion process, which may be due to the fact that the measurements were performed closer to the fuel bed.

### 3.1.2. Nitrogen species release and conversion rates for the fuels investigated

The profiles of the NO<sub>x</sub> precursors detected (see Fig. 4) above the fuel bed and the total conversion rates of the NO<sub>x</sub> precursors (see Fig. 5) are illustrated and discussed as follows. Due to the high relevance of the stoichiometric conditions in the bed (see Fig. 4) to the decomposition behaviour of the fuels, the profiles for  $\lambda_{\text{fuel bed}}$  are also illustrated and discussed.

### 3.1.3. Nitrogen species release for sawdust

The release of N started immediately (see Fig. 4a), due to a very low water content of the sawdust fuel samples. During the short H&D stage (<50 s), NO and NH<sub>3</sub> were released. The peak concentration of NO (140 ppmv) was reached immediately after ignition (at 50 s). The release of NH<sub>3</sub> started during the H&D stage and continued rising (peak value: 229 ppmv) until the middle of the P&G conversion stage (50–650 s). During this stage HCN (peak value: 126 ppmv) and NO<sub>2</sub> (peak value: 29 ppmv) were also detected. At the end of the P&G stage and during charcoal burnout (>650 s), NO was detected again in significant

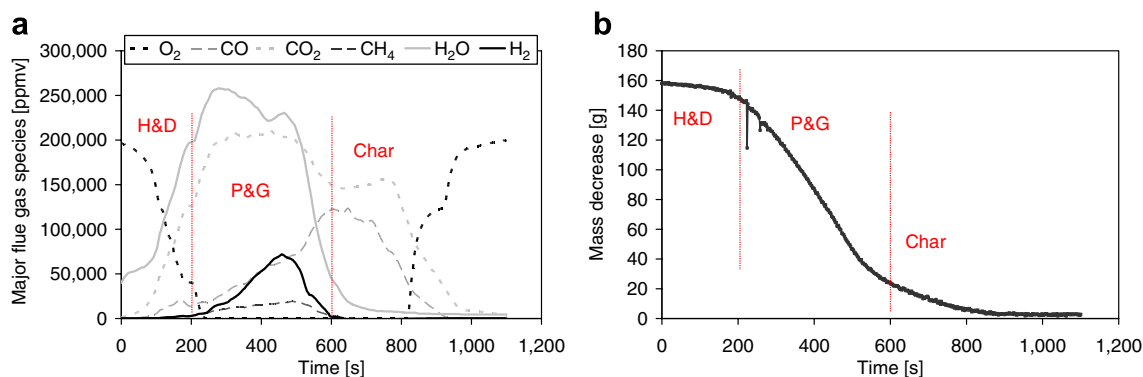


Fig. 3. Experimental results for test runs with bark. (a) Profiles of the major flue gas species (mean values); (b) Mass decrease during combustion (mean values); the data is based on three test runs; char – charcoal burnout.

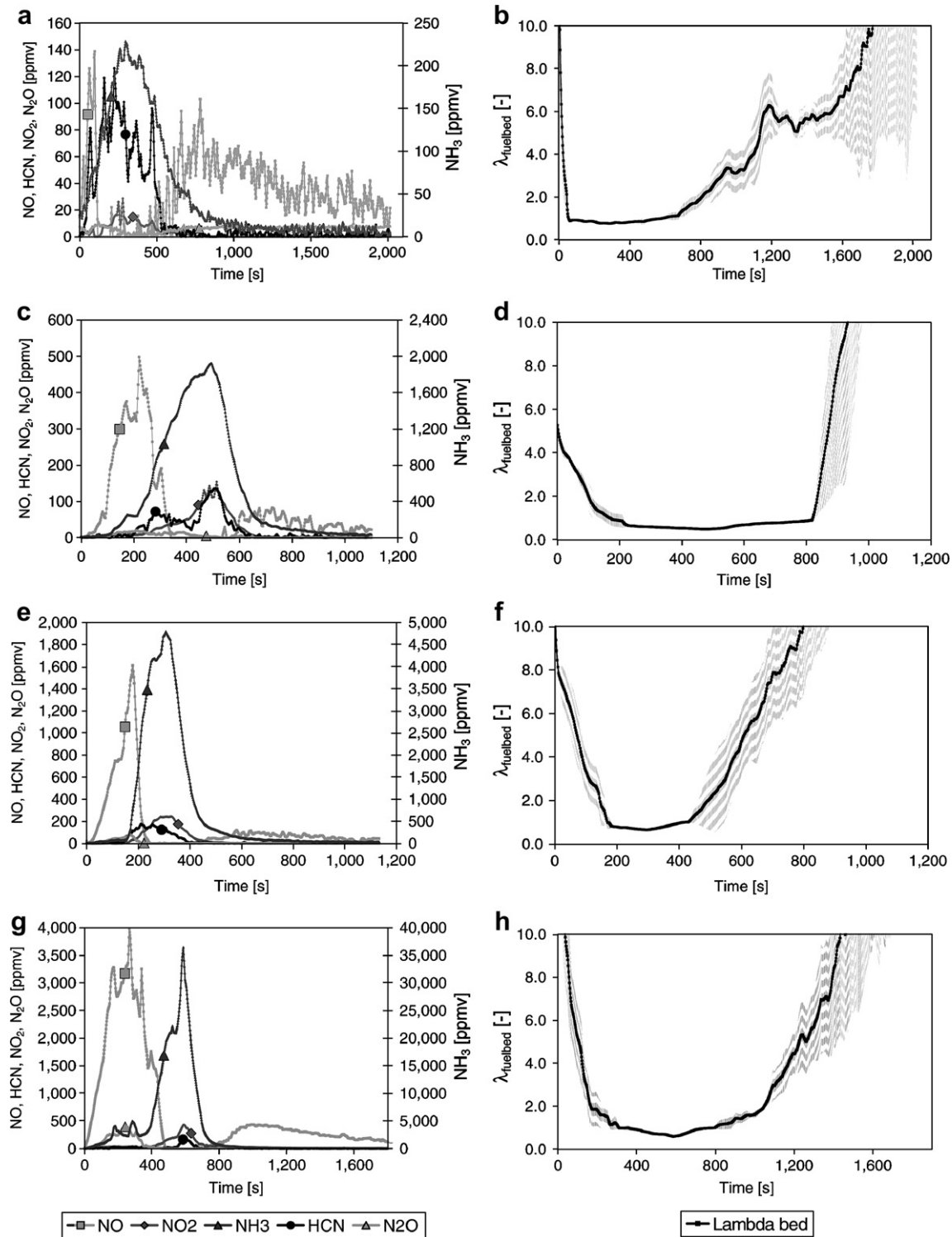


Fig. 4. Profiles of the  $\text{NO}_x$  precursors and stoichiometric air ratio above the fuel bed. Profiles of N species (mean values of three test runs) for (a) Sawdust, (c) Bark, (e) Waste wood and (g) MDF board; profiles of  $\lambda_{\text{fuel bed}}$  (Eq. (2)); mean values of three test runs and standard deviations) for (b) Sawdust, (d) Bark, (f) Waste wood and (h) MDF board; experimental conditions see Table 1; in the case of the N species profiles the illustration of the standard deviations was omitted for the purpose of clarity.

concentrations (peak value: 100 ppmv). The second NO peak is typical of biomass fuels and is caused by the released char N. During charcoal burnout oxygen becomes available again, which explains the formation of NO.  $\text{N}_2\text{O}$

was detected during almost the whole test run at a level of 11 ppmv, which may partly be caused by noise from the measurement device. The stoichiometric air ratio in the bed is illustrated in Fig. 4b. The change from air rich to

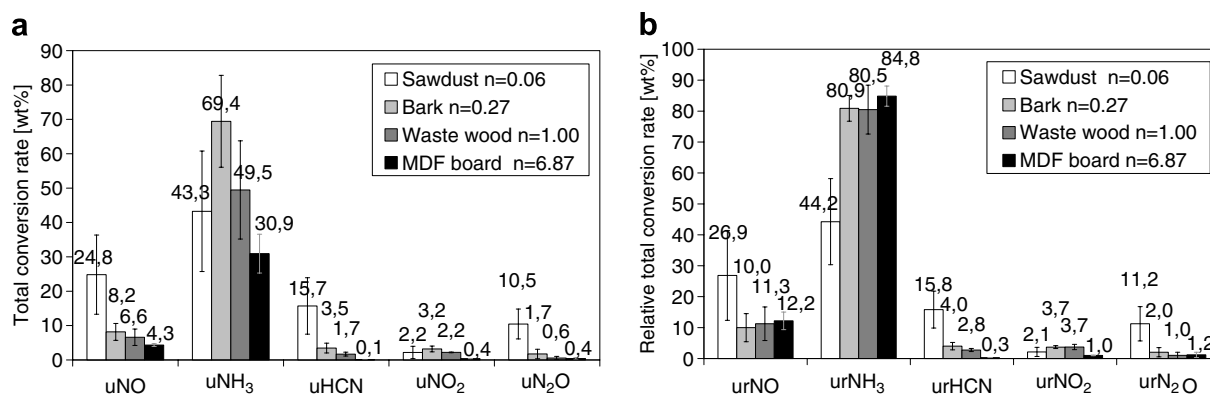


Fig. 5. Total conversion rates of relevant NO<sub>x</sub> precursors. Total N species conversion rates for the NO<sub>x</sub> precursors measured during the test runs at the lab-scale pot furnace: (a) Related to the fuel N content and (b) Related to TFN; MDF – medium density fibre; for the definition of conversion rates of the N species investigated see Chapter 2.3; the results shown are mean values (bars) with indicated standard deviations for three test runs per fuel; experimental conditions see Table 1.

air lean conditions corresponded approximately to the point of ignition (at 50 s). An air lean time period followed which lasted about one third of the total duration of the test runs and ended at approximately 750 s. The large standard deviation of  $\lambda_{\text{fuel bed}}$  in the second half of the diagram was caused by time variations in charcoal burnout during the individual test runs averaged, since the stoichiometric air ratio increased rapidly in this phase. The dominant NO<sub>x</sub> precursors were NO under air rich conditions and both NH<sub>3</sub> and HCN under air lean conditions. Sawdust was the only biomass fuel investigated that released HCN in comparable concentrations to NH<sub>3</sub> and NO during the thermal degradation of the fuel.

### 3.1.4. Nitrogen species release for bark

In the case of bark, the release of N started (see Fig. 4c) during the H&D conversion stage (<200 s). At this stage the major part of N was converted to NO (peak value: 498 ppmv). At the point of ignition (~200 s), the P&G conversion stage (200–600 s) followed. During this conversion stage NH<sub>3</sub> (peak value: 1924 ppmv) was the dominant NO<sub>x</sub> precursor, whereas comparably small amounts of HCN (peak value: 135 ppmv), NO<sub>2</sub> (peak value: 154 ppmv) and N<sub>2</sub>O (peak value: 21 ppmv) were detected. In the subsequent charcoal burnout stage (>600 s) NO (peak value: 80 ppmv) was detected again. Fig. 4d shows the stoichiometric air ratio in the bed. The change of air rich to air lean conditions corresponded approximately to the point of ignition. A long air lean time period followed until approximately 800 s, which corresponds to about 50% of the total duration of the test runs. NO was the dominant NO<sub>x</sub> precursor under air rich and NH<sub>3</sub> the dominant NO<sub>x</sub> precursor under air lean conditions.

### 3.1.5. Nitrogen species release for waste wood

For waste wood (Fig. 4e), the release of N took place almost exclusively during stages H&D (<160 s) and P&G (160–400 s). The maximum NO concentration (1610 ppmv) was detected shortly after the ignition point (~160 s). From

this point the concentration of NH<sub>3</sub> increased rapidly. The ignition point corresponded to the change of the atmospheric conditions from air rich to air lean conditions (see Fig. 4f). The air lean stage lasted approximately 300 s, i.e. about 25% of the total duration of the test runs. NH<sub>3</sub> reached a peak concentration of almost 4793 ppmv during the P&G conversion stage. The species HCN (peak value: 175 ppmv), NO<sub>2</sub> (peak value: 242 ppmv) and N<sub>2</sub>O (peak value: 79 ppmv) were detected in comparably small amounts and achieved their maxima also during the P&G stage. During charcoal burnout (>400 s), a second peak of NO was detected (120 ppmv). NO was the dominant NO<sub>x</sub> precursor under air rich and NH<sub>3</sub> the dominant NO<sub>x</sub> precursor under air lean conditions.

### 3.1.6. Nitrogen species release for MDF board

The concentrations of N species detected during the test runs with MDF board were significantly higher than for the other fuels investigated due to the higher fuel N content of MDF board (Fig. 4g). The fuel N released during the H&D stage (<160 s) was converted to NO (peak value: 3300 ppmv), NH<sub>3</sub> (peak value: 4051 ppmv) and N<sub>2</sub>O (peak value: 259 ppmv). The ignition of the fuel took place at about 160 s, which corresponded to the change from air rich to air lean conditions (see Fig. 4h). Beyond this point (P&G conversion stage from 160 to 720 s), the concentrations of NO (peak value: 3978 ppmv) and N<sub>2</sub>O (peak value: 402 ppmv) further increased but decreased again soon after the ignition. The release of NH<sub>3</sub> also increased very rapidly up to the peak value of 36,440 ppmv until the middle of the P&G stage. HCN (peak value: 178 ppmv) and NO<sub>2</sub> (peak value: 430 ppmv) were also detected during this conversion stage, but only in comparatively small amounts. The air lean conditions lasted approximately 550 s (about one third of the total duration of the test runs). During charcoal burnout (>720 s), the concentration of NO increased again to a peak concentration of 440 ppmv. NO and NH<sub>3</sub> were the dominant NO<sub>x</sub> precursors under air rich and air lean zones, respectively.

### 3.1.7. Total N conversion rates for the biomass fuels investigated

Fig. 5 shows a comparison of the total conversion rates of the N species detected during the test runs for the fuels investigated. The conversion rates related to the fuel N content are given in Fig. 5a. In the case of NO, HCN and N<sub>2</sub>O decreasing conversion rates were observed for increasing fuel N contents. The conversion rates of NH<sub>3</sub> and NO<sub>2</sub> increased from sawdust to bark, but then decreased from bark to fuels with higher fuel N contents. It can be observed that NH<sub>3</sub> was the dominant NO<sub>x</sub> precursor above the fuel bed during the test runs for bark, waste wood and MDF board. In the case of sawdust, the total fuel N released was converted mainly to NH<sub>3</sub> but also in relevant fractions to NO and HCN.

The conversion rates related to TFN are shown in Fig. 5b. In the case of NO and NH<sub>3</sub> the relative conversion rates are almost equal for MDF board, waste wood and bark (different fuel N contents and similar particle sizes). In the case of sawdust (very low fuel N content and small particles) a significantly higher relative conversion rate was observed for NO and a significantly lower relative conversion rate for NH<sub>3</sub>. In the case of HCN the relative conversion rates slightly increased with decreasing fuel N content for MDF board, waste wood and bark. Sawdust showed significantly higher relative conversion rates of HCN than the other biomass fuels investigated. The conversion rates of NO and NH<sub>3</sub> related to TFN are almost the same for bark, waste wood and MDF board (similar mean particle sizes), contrary to the conversion rates related to fuel N contents (compare Fig. 5a and b). This means that the formation of N<sub>2</sub> increases (undetected fuel N released is assumed to be N<sub>2</sub>) with increasing fuel N content. The dominance of NH<sub>3</sub> among the NO<sub>x</sub> precursors is even more strongly pronounced for the conversion rates related to TFN compared to the conversion rates related to the fuel N content (compare Fig. 5a and b). In the case of sawdust, NO and HCN were also detected in large amounts above the fuel bed. The relatively high mass fraction of N<sub>2</sub>O detected might partly be caused by the noise of the measurement system.

The correlation of the TFN conversion rates with the fuel N contents of the biomass fuels investigated is shown in Fig. 6, which indicates that the TFN conversion rate increases with decreasing fuel N content. This behaviour was also observed by Salzmann and Nussbaumer [3],

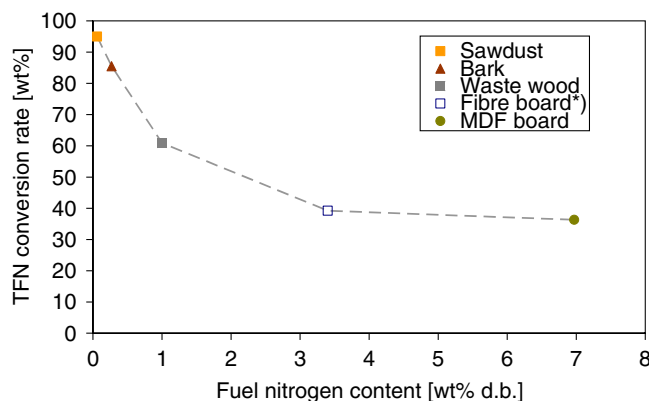


Fig. 6. Correlation of TFN conversion rates with fuel N contents. Fibre board. Source: [12].

Weissinger [4] and Winter et al. [10]. It is believed that the fraction of N<sub>2</sub> formed increases with rising concentrations of N species in the flue gas.

### 3.1.8. Discussion of the experimental results

Volatile N (vol N) and char N were determined separately for all fuels investigated. The N species released during the pyrolysis phase were summed up and related to the cumulated N species released during charcoal burnout. It must be stated that the ratios of this calculation should be understood as approximations due to overlapping conversion phases. It was observed that in general the ratio of vol N/char N decreased from MDF board to sawdust, which means that the lowest mass fraction of N was retained in the char for MDF board and the highest for sawdust (see Table 3). This leads to the conclusion that the ratio of vol N/char N increases with rising fuel N content. Leppälähti [7] also observed an increase in the fraction of char N with decreasing fuel N content.

As an exception, the vol N/char N ratio for bark was higher than for waste wood despite a lower fuel N content. The mode of occurrence in the fuel might play a role in this case; thus bark may contain more N bound in proteins (higher volatility) than in aromatic compounds compared to waste wood. Amine and quaternary N are believed to be released mainly as NH<sub>3</sub> [6,9], while pyridinic and pyrrolic N are believed to be released mainly as HCN [6,9] from biomass fuels. During this study the mode of occurrence of N was not analysed and therefore no further statement can be made.

Table 3  
TFN conversion rate (pyrolysis phase) versus maximum temperature for selected test runs

Fuel	Bark			MDF board		
	Experiment 1	Experiment 2	Experiment 3	Experiment 1	Experiment 2	Experiment 3
Max <i>T</i>	997	1075	1179	1112	974	958
uTFNp	0.84	0.63	0.87	0.35	0.31	0.25
uTFCp	0.76	0.62	0.75	0.69	0.67	0.65

Max *T* – maximum temperature observed in the pyrolysis zone of the fuel bed; uTFNp – conversion rate of TFN released during pyrolysis phase; uTFCp – conversion rate of TFC (total fixed carbon – mainly CO, CO<sub>2</sub>, CH<sub>4</sub>) released during pyrolysis.

Table 3 shows the relation between the maximum temperature in the fuel bed during pyrolysis and N release. In the case of bark no clear trend concerning the influence of temperature on N release can be observed, but a correlation between N and C release is apparent. In the case of MDF board the fuel N as well as fuel C release during the pyrolysis phase increased with raising maximum temperatures.

Thus, temperature seems to influence N release indirectly by its influence on the release of the volatile fuel fraction since the ratio between volatiles and char is temperature dependent and the fraction of volatiles increases with increasing temperature. Further investigations concerning the influence of temperature on N release and N species formation are needed in order to be able to give a more detailed statement.

Large differences were observed between the concentration levels of the  $\text{NO}_x$  precursors ( $\text{NO}$ ,  $\text{NH}_3$ ,  $\text{HCN}$ ,  $\text{NO}_2$  and  $\text{N}_2\text{O}$ ) for the four fuels investigated. The most significant deviations were found for  $\text{NH}_3$ . The maximum concentrations of  $\text{HCN}$  were approximately in the same range for all four fuels. The concentrations of the  $\text{NO}_x$  precursors are strongly dependent on the fuel N content, i.e. the highest concentrations were measured for MDF board and the lowest for sawdust. The trend for the TFN conversion rates is exactly contrary to the trend for  $\text{NO}_x$  precursor concentrations since the highest conversion of the fuel N to  $\text{NO}_x$  precursors occurred for sawdust while the lowest conversion was observed for MDF board.

The concentration levels of the different  $\text{NO}_x$  precursors also varied significantly. The dominant N flue gas species were  $\text{NO}$  under oxygen rich and  $\text{NH}_3$  under fuel rich conditions for all fuels investigated. The global results (N species conversion rates) confirm the previously findings. This leads to the conclusion that the formation of N flue gas species is dependent on the air ratio. In the preceding work of Weissinger et al. [12]  $\text{NO}$  and  $\text{NH}_3$  were measured in concentrations comparable to the results obtained in this work. Furthermore, the concentration profiles of  $\text{NO}$  and  $\text{NH}_3$  detected by Samuelsson et al. [11] are in qualitative agreement with the data presented in this work.

$\text{HCN}$ ,  $\text{NO}_2$  and  $\text{N}_2\text{O}$  were not detected in significant concentrations above the fuel bed, with the exception of  $\text{HCN}$  in the case of sawdust. Contrary to the present work, no  $\text{HCN}$  was detected by wet chemical analysis in the gas phase during the experiments carried out in a pre-

vious study by Weissinger et al. [12]. No explanation for this was found in the present study. Furthermore, Samuelsson et al. [11] also found no  $\text{HCN}$  but also no  $\text{NO}_2$  and  $\text{N}_2\text{O}$  in the gas phase during the combustion of pelletised sawdust and bark, probably due to the relatively high detection limits of the measuring devices used. In the study carried out by Keller [5] at an under-stoker burner (fuel: fibre board), large amounts of  $\text{HCN}$  were detected above the fuel bed in concentrations close to those of  $\text{NH}_3$ . In the same study it was observed that the fraction of  $\text{HCN}$  increased with decreasing air ratios and fuel N contents. Both trends were observed during this study as well.

As mentioned before,  $\text{HCN}$  was an important  $\text{NO}_x$  precursor besides  $\text{NH}_3$  under air lean conditions in the case of sawdust. This fact is also confirmed by the global results since  $\text{HCN}$  strongly contributed to the total fuel N released besides  $\text{NO}$  and  $\text{NH}_3$ . Furthermore,  $\text{HCN}$  became more important due to significantly lower concentrations of  $\text{NO}$  and particularly  $\text{NH}_3$  in sawdust compared to the other fuels investigated. The reason for this may be the small particle size of sawdust. For the fuels bark, waste wood and MDF board (comparable fuel particle sizes, see Table 4)  $\text{HCN}$  concentrations were not significant above the fuel bed compared to  $\text{NH}_3$ . Hansson et al. [9] and Winter et al. [10] stated that more  $\text{HCN}$  is formed in the case of smaller particles due to higher heating rates and shorter residence times of the compounds released in the particles. Further investigations on the influence of particle size on N release and N species formation are thus recommended in the future.

The  $\text{HCN}/\text{NH}_3$  ratio decreased from sawdust to MDF board (see Table 4). The reasons for this are most probably increasing fuel N contents and decreasing ratios of H/N and O/N in the fuel under combustion conditions. The very high ratio of  $\text{HCN}/\text{NH}_3$  in the case of sawdust is most probably intensified by the small fuel particles (see Table 4) compared to the other fuels as explained earlier. This is in contrary to previous studies [1,3,10]; while the review of Glarborg et al. and the study of Salzmann and Nussbaumer was based on inert conditions, the study of Winter et al. was based on combustion conditions as well. Why the trend observed is opposite to the literature is not understood so far.

The amount of OH radicals in the gas phase is believed to be an important reactant for the N species, which

Table 4  
Relevant N release parameters of the biomass fuels investigated

Fuel	$n$ (wt% d.b.)	vol N/char N (-)	H/N (-)	$\text{HCN}/\text{NH}_3$ (-)	O/N (-)	$\text{N}_2\text{O}/\text{NO}$ (-)	Mean $d_p$ (mm)
Sawdust	0.06	1.6	1529	0.36	645	0.27	0.3
Bark	0.27	13.8	288	0.05	130	0.21	3.0
Waste wood	1.00	11.2	83	0.03	38	0.09	2.8
MDF board	6.87	24.9	13	0.00	5	0.09	2.7

$n$  – nitrogen content; vol N – N in volatiles; char N – N in charcoal; H/N – ratio of hydrogen to nitrogen;  $\text{HCN}/\text{NH}_3$  – ratio of  $\text{HCN}$  to  $\text{NH}_3$ ; O/N – ratio of oxygen to nitrogen;  $\text{N}_2\text{O}/\text{NO}$  – ratio of  $\text{N}_2\text{O}$  to  $\text{NO}$ ; all ratios on molar basis;  $d_p$  – particle diameter; mean  $d_p$  –  $d_p$  on the basis of particle number.

increases with higher O/N ratios [2,6]. OH radicals in the gas phase may also be formed from H<sub>2</sub>O released, making the moisture content of a biomass fuel a potentially important parameter. Further investigations on the influence of moisture content on N release and N species formation are thus needed.

In general, the N<sub>2</sub>O concentrations measured were very low compared to NO and NH<sub>3</sub> for all fuels investigated. However, in the air rich sections, primarily in the case of waste wood and MDF board, the N<sub>2</sub>O detected followed the NO profile, although at a significantly lower level. This leads to the conclusion that NO might play an important role in the formation of N<sub>2</sub>O.

In addition, the N<sub>2</sub>O/NO ratio decreased from sawdust to MDF board with a decreasing O/N ratio as can be seen in Table 4. This is in agreement with the review of Glarborg et al. [1] and the study of Hämäläinen and Aho [6], where it was stated that a higher O/N ratio leads to increased formation of N<sub>2</sub>O. Further investigations on the formation of N<sub>2</sub>O and its precursors need to be performed in the future.

Furthermore, it was stated by Kilpinen and Hupa (kinetic modelling study) [20], Hämäläinen and Aho [6] and Winter et al. [10] that HCN is a major precursor for N<sub>2</sub>O formation. Contrary to this finding, HCN and N<sub>2</sub>O do not appear to correlate in the present study. However, the previous studies were done under fluidised bed conditions and Kilpinen and Hupa [20] stated that a significant fraction of HCN is oxidised to N<sub>2</sub>O under air rich

conditions. This may explain the difference to the present study since HCN was released under air lean conditions and, therefore, N<sub>2</sub>O was scarcely formed during the experiments.

### 3.2. Release functions

The release functions (see Chapter 2.3) derived for the solid biomass fuels sawdust, bark, waste wood and MDF board are presented in this chapter. The calculation results are compared with the measurement results in detail, taking sawdust as an example. The predicted profiles of the N species NO, NH<sub>3</sub> and HCN form the boundary conditions for the subsequent CFD gas phase calculations of N species in the flue gas. Following on from this the total conversion rates measured and calculated for NO, NH<sub>3</sub> and HCN are discussed. Finally, the compilation of the release functions is presented for sawdust, bark, waste wood and MDF board. The release functions were derived according to the methodology described in chapter 2.3.

Fig. 7 shows the relevant results of the comparison between calculations and measurements for sawdust. It gives the calculated and measured profiles over time for  $\lambda_{\text{fuel bed}}$  as well as for the flue gas concentrations of NO, NH<sub>3</sub> and HCN immediately above the fuel bed. The calculated  $\lambda_{\text{fuel bed}}$  values are in a good qualitative agreement with the measured values (see Fig. 7a). Deviations are due to the lack of detection of tar and higher hydrocarbons in the main release zone as well as due to variations

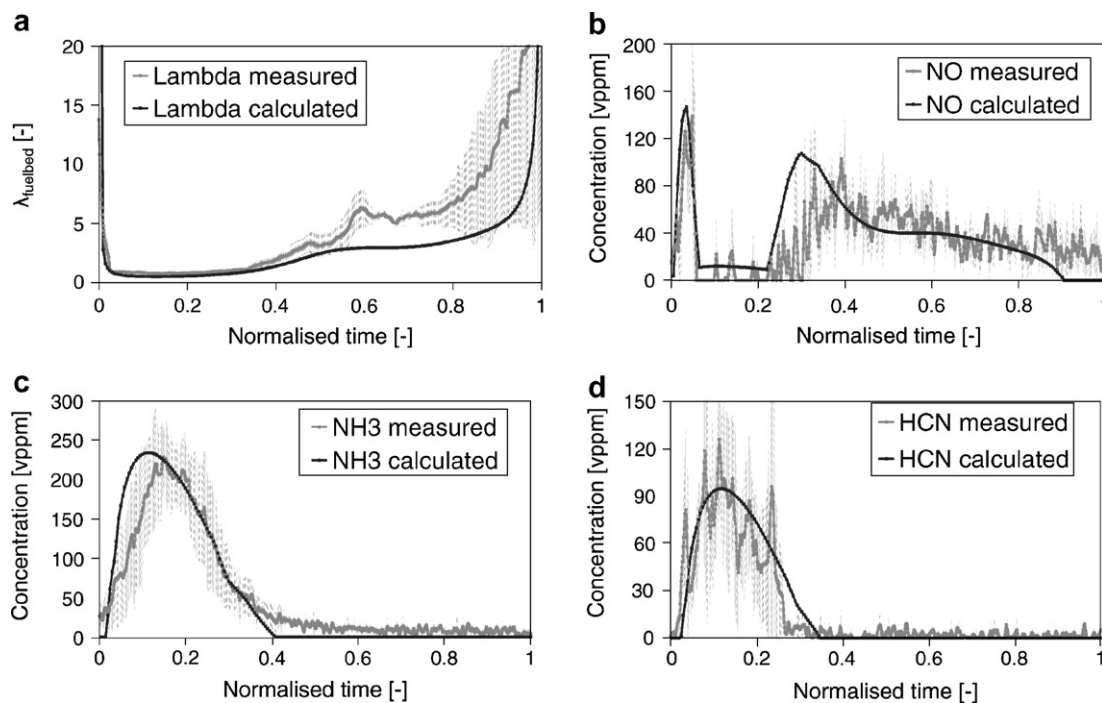


Fig. 7. Comparison of results for  $\lambda_{\text{fuel bed}}$  calculated and measured and for the NO<sub>x</sub> precursors NO, NH<sub>3</sub> and HCN released for sawdust. (a) Profiles of  $\lambda_{\text{fuel bed}}$ , (b) Profiles of the flue gas concentrations of NO, (c) NH<sub>3</sub> and (d) HCN; concentrations are related to volume ppm (wet base); fuel sawdust:  $n = 0.06$  wt%(d.b.),  $w = 0.1$  wt%(w.b.); the measured results shown are mean values of three test runs with the standard deviations indicated; normalised time – referred to duration of test runs.

between the measured and calculated release profiles of the fuel components. The high standard deviations of the measured profiles in the last third of the test runs are due to differences (e.g. test run duration and slope of oxygen concentration) between the single test runs averaged. A good qualitative and quantitative agreement between measurements and calculations was observed for the concentration profile of NO (see Fig. 7b). However, the second NO peak during the charcoal burnout stage is slightly shifted to earlier times, due to the rapid change of  $\lambda_{\text{fuel bed}}$  in this region. An improvement in prediction of the second NO peak leads to a poorer prediction of the first peak (H&D stage) and vice versa. For this reason, a solution, which gives a reasonable result for both peaks, was preferred. Furthermore, the calculated concentration profiles for  $\text{NH}_3$  (see Fig. 7c) and HCN (see Fig. 7d) showed a good agreement with the measured profiles. The concentration of  $\text{NH}_3$  is over-predicted in the early release stages, which can be explained by the rapid change of  $\lambda_{\text{fuel bed}}$  in this zone.

A qualitative agreement (not shown here) between calculated and measured profiles of  $\lambda_{\text{fuel bed}}$  was also found for bark, waste wood and MDF board. Deviations between these profiles were observed during the conversion processes especially at positions of rapid  $\lambda_{\text{fuel bed}}$  changes as in the case of sawdust. The quantitative deviations observed were most probably due to the lack of measurements of tars and larger hydrocarbons in the case of the  $\lambda_{\text{fuel bed}}$  calculated as well as deviations between the measured and calculated release profiles. Considering the linear approach used for the determination of the release func-

tions, the calculated results of the local  $\text{NO}_x$  precursor concentrations are in a satisfactory agreement with those measured for bark, waste wood and MDF board.

The comparison of calculated and measured total conversion rates of NO,  $\text{NH}_3$  and HCN for all solid biomass fuels investigated is given in Fig. 8. The diagram shows a very good agreement for all three  $\text{NO}_x$  precursors with deviations between calculated and measured data below 3%. It can be concluded that an accurate prediction of the total conversion rates is easier to achieve than the prediction of the concentration profiles of the  $\text{NO}_x$  precursors as was previously illustrated for sawdust. Consequently, local concentration deviations of the  $\text{NO}_x$  precursors might occur during the subsequent CFD gas phase calculations due to the fact mentioned previously. Most important is the major release zone of the biomass fuel bed (mainly the P&G conversion stage), which appears to be well predicted. Slight deviations seem to occur for the surrounding areas, but they are less significant due to the lower mass flows released there. The results of the N species release model should be seen as sufficient approximation for N release prediction in biomass grate furnaces. It will be necessary to investigate the influence of the deviations of the N species profiles from the N species release model on the CFD gas phase calculations in the future.

The parameters of the N species release functions derived for the fuels sawdust, bark, waste wood and MDF board are summarised in Table 5. The release function parameters presented are utilised in combination with the release functions for N species formation (Eq. (1)) in line with the procedure described in chapter 2.3. According

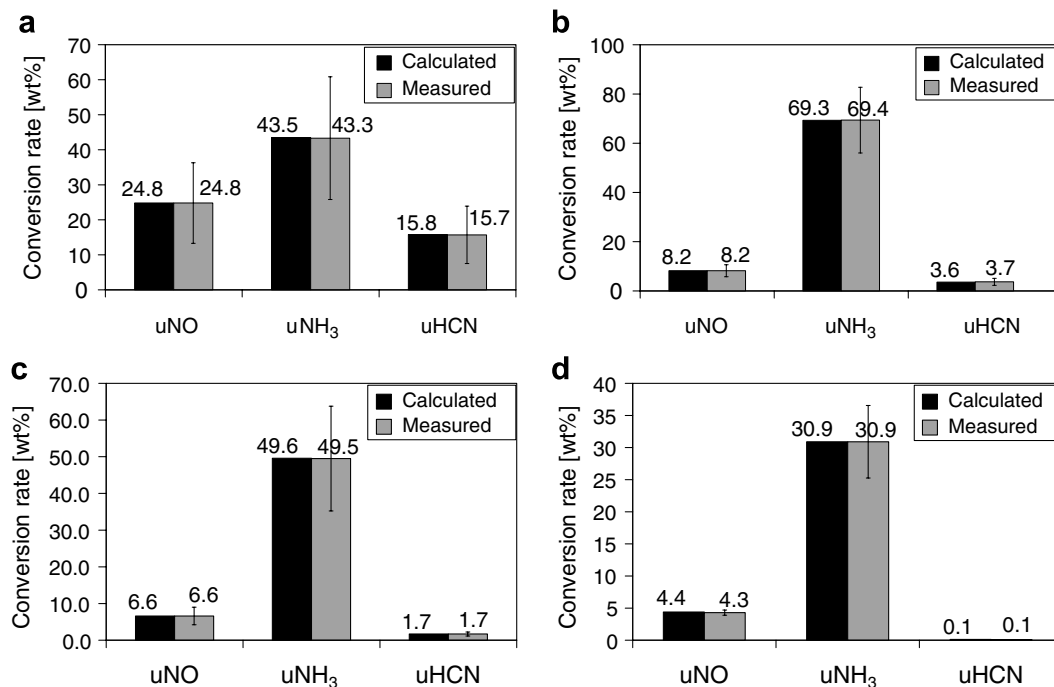


Fig. 8. Comparison of calculated and measured conversion rates for the relevant  $\text{NO}_x$  precursors NO,  $\text{NH}_3$  and HCN. (a) Sawdust, (b) Bark, (c) Waste wood and (d) MDF board; the measurement results shown are mean values (bars) of three test runs per fuel with standard deviations.

Table 5  
Derived parameters for the release functions of relevant N species

Fuel	$n$ (wt% d.b.)	$k_{\text{NO}}$ (–)	$d_{\text{NO}}$ (–)	$k_{\text{NH}_3}$ (–)	$d_{\text{NH}_3}$ (–)	$k_{\text{HCN}}$ (–)	$d_{\text{HCN}}$ (–)
Sawdust	0.06	3.30	–1.88	–0.62	0.91	–0.49	0.49
Bark	0.27	0.85	–0.44	–2.12	1.94	–0.15	0.12
Waste wood	1.00	0.90	–0.70	–0.91	1.20	–0.03	0.04
MDF board	6.87	0.15	–0.10	–0.94	0.94	–0.06	0.03

$n$  – fuel N content;  $k_i$  – slope for species  $i$ ;  $d_i$  –  $y$ -intercept for species  $i$ .

to the results shown above, the predicted concentration profiles of NO, NH<sub>3</sub> and HCN are in reasonable agreement and the total conversion rates of NO, NH<sub>3</sub> and HCN are in very good agreement with the measurement results achieved at the lab-scale reactor.

The release functions derived provide the concentration profiles of NO, NH<sub>3</sub> and HCN released from the fuel bed as a function of the local stoichiometric air ratio in the fuel bed and the fuel N content. The elemental balance of N is closed by the N<sub>2</sub> formed. This N species release model can be implemented in any packed bed combustion model and can be applied to the prediction of N species release from the fuel bed for the fuels investigated.

The purpose of the N species release model presented is to provide a subsequent CFD gas phase combustion model with the boundary conditions required (concentration profiles of NO, NH<sub>3</sub> and HCN) for the purpose of NO<sub>x</sub> emission predictions of real-scale biomass grate furnaces as well as for the development of design rules for real-scale low-NO<sub>x</sub> biomass grate furnaces.

However, this compilation of release functions is only valid for the fuels investigated with the given fuel N contents, particle sizes and moisture contents. It is possible to interpolate the release function parameters for an unknown fuel N content between known data sets for a specific kind of fuel. This procedure was developed in the work of Widmann [16] where a description can be found. The investigation of the influence of fuel particle size and moisture content on N release and N species formation is one task which needs to be investigated further in future. No clear statement concerning the influence of these two parameters can thus be given up to now.

The calculated concentration profiles deviate slightly from the measurements (see Fig. 7), while the total conversion rates of the different N species (see Fig. 8) are predicted accurately. Most important is the major release zone of the biomass fuel bed (mainly the P&G conversion stage), which seems to be well predicted. Slight deviations seem to occur for the surrounding areas, but they are less significant due to the lower mass flows released there. Consequently, the results predicted by the N species release model can be seen as a sufficient approximation of the real conditions in biomass grate furnaces.

Furthermore, it has to be stated that the temperature is not explicitly included in the release functions, hence, no kinetic relations are considered since the reaction conditions are based on the experimental conditions. Following,

an option to further improve the N species release model developed would be the consideration of kinetic relations in the release equations.

The N species release model developed has already been implemented in an empirical packed bed combustion model and was utilised in combination with a CFD gas phase combustion tool. CFD calculations of the NO<sub>x</sub> emissions of a biomass grate combustion plant were performed in the study of Scharler et al. [17] following this modelling approach. The results showed a good agreement with NO<sub>x</sub> measurements at boiler outlet. The N release model in combination with a packed bed combustion model works well and provides the boundary conditions for the CFD calculations concerning the N species release.

The applicability and limitations of the experimental approach forming the basis for the N species release model are summarised in the following. The lab-scale reactor is designed to simulate packed bed combustion. The simplifying assumptions of the lab-scale reactor are (1) the speed of the packed bed on the grate is constant, (2) the diffusional transport and mixing effects in the direction of the grate can be neglected compared to the transport of the fuel along the grate and hence, (3) in dependence on a certain residence time, any particle can be related to a position on the grate according to the conversion progress. Furthermore, the so-called real-scale effects such as channelling and flue gas strains during the combustion process occur to a smaller extent in the lab-scale reactor. Moreover, the particle size of biomass fuels utilised at real-scale biomass grate furnaces is larger in most cases and the simulation of flue gas recirculation in the lab-scale reactor is restricted. In this context also the results of the N species release model should be seen as sufficient approximation of the most relevant N species released from a biomass fuel bed. The general applicability of the lab-scale results to real-scale grate combustion is discussed in the study of Stubenberger et al. [21]. The main conclusions are that the thermal conversion process, the qualitative comparison of flue gas species released and the fuel N release are sufficiently similar.

#### 4. Summary and conclusions

Experimental data of the combustion and release behaviour for a selection of solid biomass fuels were gained through several measurement campaigns in a lab-scale pot furnace reactor (packed bed batch reactor). These

experimental data include the concentration profiles of the N containing species NO, NH<sub>3</sub>, HCN, NO<sub>2</sub> and N<sub>2</sub>O over time. The measured profiles were utilised for the derivation of release functions for the most relevant NO<sub>x</sub> precursors measured. The fuels investigated were sawdust, bark, waste wood and MDF board, thus covering a broad range of woody biomass fuels.

Vol N and char N release were investigated separately for all fuels considered and it was observed that the fraction of vol N increased with increasing fuel N content. The mode of occurrence in the fuel might play a role in this case; the fraction of vol N might thus be higher for fuels which contain more N bound to proteins (higher volatility) than in aromatic compounds. Furthermore, the influence of temperature on the ratio between volatiles and char of the fuel is important, since it also affects the ratio between vol N and char N.

It was found that the fuel N content and the stoichiometric air ratio are major influencing parameters on the time dependent release behaviour and the total conversion rates of NO<sub>x</sub> precursors. The maximum concentrations of the N species detected during the test runs increased with rising fuel N content, whereas the TFN conversion rates of the woody biomass fuels investigated increased with decreasing fuel N content. For example, almost complete conversion of fuel N to TFN was observed for sawdust.

Furthermore, NO was found to be the major NO<sub>x</sub> precursor released from the fuel bed under air rich conditions and the N species NH<sub>3</sub> (and HCN in the case of sawdust) under air lean conditions. The reason for the importance of HCN in the case of sawdust may be due to the low fuel N content and the small fuel particles. HCN was detected in negligible concentrations for bark, waste wood and MDF board. The concentrations of NO<sub>2</sub> and N<sub>2</sub>O measured above the fuel bed were of no relevance for the fuels investigated. Furthermore, it was observed that NO might play a role in N<sub>2</sub>O formation in air rich sections, whereas no correlation was found between HCN and N<sub>2</sub>O.

The results obtained for the total conversion rates of N species confirmed the observations of the N species concentration profiles. Furthermore, NH<sub>3</sub> contributed the largest mass fraction of all N flue gas species for all fuels investigated, although also HCN and NO contributed large mass fractions in the case of sawdust.

It was observed that the HCN/NH<sub>3</sub> ratio decreased with increasing fuel N contents and with decreasing H/N and O/N ratios. The N<sub>2</sub>O/NO ratio decreased from sawdust to MDF board (increasing fuel N content) and with decreasing O/N ratio, which may explain the relatively high emissions of N<sub>2</sub>O in the case of sawdust.

Release functions for the solid biomass fuels investigated were generated and compiled in a database. Under comparable conditions, the concentration profiles measured (pot furnace experiments) and calculated (empirical packed bed model) over time were in reasonable agreement; the calculated and measured total conversion rates for the main NO<sub>x</sub> precursors matched very well. Consequently, the

presented N species release model allows the total conversion rates, i.e. the total emissions of the NO<sub>x</sub> precursors to be predicted more accurately than the concentration profiles over time. This means that local concentration deviations of the NO<sub>x</sub> precursors might occur in the subsequent CFD gas phase calculations. The results of the N species release model can be seen as sufficient approximation and a valuable basis for the prediction of NO<sub>x</sub> in real-scale biomass grate furnaces. The release functions derived are valid for the biomass fuels investigated with the given fuel N contents, particle sizes and moisture contents.

In summary, this work provides a N species release model, which is based on empirical data for packed bed biomass combustion. For each fuel investigated, the release function parameters derived for the linear release functions provide conversion rates of the fuel N as a function of the local stoichiometric air ratio in the fuel bed and the fuel N content. However, it should be kept in mind that the model is not based on any kinetic relations, due to the fact that there is no explicit temperature dependence included.

The N species release model presented can be applied in any packed bed combustion model in order to obtain concentration profiles for NO, NH<sub>3</sub> and HCN (boundary conditions) for a subsequent CFD gas phase combustion model in order to predict N species release from the fuel bed in a real-scale biomass grate furnace. This is a basis and a relevant step towards a cost-efficient design and optimisation of biomass grate furnaces with respect to NO<sub>x</sub> emission reduction.

## References

- [1] Glarborg P, Jensen AD, Johnsson JE. Fuel nitrogen conversion in solid fuel fired systems. *Prog Energy Combust Sci* 2003;29:89–113.
- [2] Samuelsson JI. Conversion of nitrogen in a fixed burning biofuel bed. Thesis for the degree of licentiate of engineering. Chalmers University of Technology, Göteborg, Sweden, 2006.
- [3] Salzmann R, Nussbaumer T. Fuel staging for NO<sub>x</sub> reduction in biomass combustion: experiments and modeling. *Energ Fuel* 2001;15:575–82.
- [4] Weissinger A. Experimentelle Untersuchungen und reaktionskinetische Simulationen zur NO<sub>x</sub>-Reduktion durch Primärmaßnahmen bei Biomasse-Rostfeuerungen. PhD thesis. Graz University of Technology, Graz, Austria, 2002.
- [5] Keller R. Primärmaßnahmen zur NO<sub>x</sub>-Minderung bei der Holzverbrennung mit dem Schwerpunkt der Luftstufung. Forschungsbericht Nr. 18, 1994. Laboratory for Energy Systems (Ed.), ETH Zürich, Switzerland, 1994.
- [6] Hämäläinen JP, Aho MJ. Effect of fuel composition on the conversion of volatile solid fuel-N to N<sub>2</sub>O and NO. *Fuel* 1995;74:1922–4.
- [7] Leppälähti J. Formation of NH<sub>3</sub> and HCN in slow-heating-rate inert pyrolysis of peat, coal and bark. *Fuel* 1995;74:1363–8.
- [8] Zhou J, Masutani SM, Ishimura DM, Turn SQ, Kinoshita CM. Release of fuel-bound nitrogen during biomass gasification. *Ind Eng Chem Res* 2000;39:626–34.
- [9] Hansson K, Samuelsson J, Tullin C, Åmand LE. Formation of HNCO, HCN and NH<sub>3</sub> from the pyrolysis of bark and nitrogen-containing model compounds. *Combust Flame* 2004;137:265–77.
- [10] Winter F, Wartha C, Hofbauer H. NO and N<sub>2</sub>O formation during the combustion of wood, straw, malt waste and peat. *Bioresour Technol* 1999;70:39–49.

- [11] Samuelsson J, Rönnbäck M, Leckner B, Tullin C. Conversion of fuel nitrogen during combustion of biofuel in a fixed bed – measurements inside the bed. In: Proceedings of the international conference on science in thermal and chemical biomass conversion, Victoria, BC, Canada, 2004.
- [12] Weissinger A, Fleckl T, Obernberger I. In-situ FT-IR spectroscopic investigations of species from biomass fuels in a laboratory-scale combustor: the release of nitrogenous species. *Combust Flame* 2004;137:403–17.
- [13] Zhou H, Jensen AD, Glarborg P, Kavaliauskas A. Formation and reduction of nitric oxide in fixed-bed combustion of straw. *Fuel* 2006;85:705–16.
- [14] Obernberger I, Widmann E, Scharler R. Entwicklung eines Abbrandmodells und eines  $\text{NO}_x$ -Postprozessors zur Verbesserung der CFD-Simulation von Biomasse-Festbettfeuerungen. *Berichte aus Energie- und Umweltforschung* No. 31/2003, Ministry for Transport, Innovation and Technology (Ed.), Vienna, Austria, 2003.
- [15] Widmann E, Scharler R, Stubenberger G, Obernberger I. Release of  $\text{NO}_x$  precursors from biomass fuel beds and application for CFD-based  $\text{NO}_x$  postprocessing with detailed chemistry. In: Proceedings of the 2nd world conference and exhibition on biomass for energy, industry and climate protection, vol. II, ISBN 88-89407-04-2, ETA-Florence (Ed.), Rome, Italy, 2004, p. 1384–87.
- [16] Widmann E. Modellbildung zum Abbrandverhalten von Biomasse unter besonderer Berücksichtigung der N-Freisetzung am Beispiel einer Rostfeuerung. M.Sc. thesis, Graz University of Technology, Graz, Austria, 2002.
- [17] Scharler R, Widmann E, Obernberger I. CFD modelling of  $\text{NO}_x$  formation in biomass grate furnaces with detailed chemistry. In: Proceedings of the international conference on science in thermal and chemical biomass conversion, Victoria, BC, Canada, 2004.
- [18] Fleckl T. Verbrennungsdiagnostik an Biomasserostfeuerungen mittels FT-IR in-situ Absorptionsspektroskopie. PhD thesis, Graz University of Technology, Graz, Austria, 2001.
- [19] Scharler R. Entwicklung und Optimierung von Biomasse-Rostfeuerungen durch CFD-Analyse. PhD thesis, Graz University of Technology, Graz, Austria, 2001.
- [20] Kilpinen P, Hupa M. Homogeneous  $\text{N}_2\text{O}$  chemistry at fluidized bed combustion conditions: a kinetic study. *Combust Flame* 1991;85:94–104.
- [21] Stubenberger G, Scharler R, Obernberger I. Nitrogen release behavior of different biomass fuels under lab-scale and pilot-scale conditions. In: Proceedings of the 15th European biomass conference and exhibition, ETA-Florence (Ed.), Berlin, Germany, 2007.